Slot Synchronization of WDM Packet-Switched Slotted Rings: the WONDER Project

Stefano Bregni*, *Senior Member, IEEE,* Diego Carzaniga*,
Roberto Gaudino**, *Member, IEEE,* Achille Pattavina*, *Senior Member, IEEE*

*Politecnico di Milano, Dept. of Electronics and Information, Piazza Leonardo Da Vinci 32, 20133 Milano, ITALY
Tel.: +39-02-2399.3503 – Fax: +39-02-2399.3413 – E-mail: bregni@elet.polimi.it
**Politecnico di Torino, Dept. of Electronics, Corso Duca degli Abruzzi 24, 10129 Torino, ITALY
Tel.: +39-011-5644172 – Fax: +39-011-5644099 – E-mail: gaudino@polito.it

***Abstract* — The WONDER project aims at designing and building a WDM packet-switched slotted ring network, with tunable transmitters and fixed receivers. An experimental prototype is under development at the laboratories of Politecnico di Torino. In this paper, we study two different strategies of slot synchronization for such networks: in the former, a slot synchronization signal is transmitted by the master station on a dedicated control wavelength; in the latter, slave nodes achieve slot synchronization aligning on data packets received from the master. Emphasis has been given to the architecture of the WONDER network. The performance of the two synchronization strategies, in terms of packet collision probability, has been evaluated by simulation. The technique based on transmitting a timing signal on a dedicated control wavelength resulted in achieving a better performance, although being more expensive due to need of an additional wavelength. However, the technique based on aligning on data packets received from the master should be not discarded, although attaining lower timing stability, especially if limiting the number of wavelengths and receivers is a strong requirement.**

***Index Terms* — Metropolitan area networks, optical networks, phase locked loops, synchronization, WDM.**

I. Introduction

WDM packet-switched ring architectures based on tunable transmitters and fixed receivers receive significant interest in the optical networking area [1], owing to their good balance between optical and electronic complexity [2][3]. Such architectures have been studied under different aspects [4][5] and applied in several experimental projects, for instance Hornet [6] and RingO [7]. More recently, the WONDER (WDM Optical Network Demonstrator over Rings) project [8][9] further develops the RingO design, with the ambitious goal of building and testing an experimental optical ring network capable of carrying real IP traffic.

These ring networks are based on synchronous time-slotted operation on all wavelengths, with typical slot duration in the microsecond range. Similar architectures have been analyzed already under many aspects in several papers. Nevertheless, to our knowledge, possible techniques for slot synchronization of such networks have not been investigated and their performance has not been evaluated yet.

In the laboratories of Politecnico di Torino, the WONDER prototype is currently under experimental development. Among the various challenging tasks of this project, we investigated possible time-slot synchronization techniques, suitable for application in this project as well as in similar networks.

In this paper, we report some of the most interesting results obtained in this work. We studied two different strategies of slot synchronization in these types of ring architectures, with emphasis on the WONDER network: in the former, a slot synchronization signal is transmitted by the master station on a dedicated control wavelength; in the latter, slave nodes achieve slot synchronization aligning on data packets received from the master.

The paper is organized as follows. An essential review of the WONDER architecture is given in Section II. Section III presents the network model and the relevant assumptions. Sections IV and V detail the two synchronization techniques and report some performance evaluation results.

II. The WONDER Architecture

WONDER is a research project [8][9] focused on demonstrating the feasibility of a ring packet-switched optical MAN, using state-of-the-art, but commercially available, optoelectronic technology. It is a development of the RingO design [7].

The WONDER network topology and node architecture, shown in Fig. 1, are based on two fiber rings connecting N nodes. One of the rings (TX) is devoted to data transmission, while the other (RX) to data reception. The WDM network is designed according to the tunable-transmitters/fixed-receivers paradigm [2][4]. The transmission of packets is time-slotted and synchronized on all wavelengths.

The two rings are physically interconnected by an optical shortcut, which can be placed at any node in the network. This shortcut, key to the WONDER fault-recovery capability [10], is realized by closing an optical loopback between the TX and RX rings at the output of a node. Thus, the resulting topology can be also viewed as a folded bus, on which each node has two connections in two distinct points.

One wavelength may be dedicated to carry control signals (e.g., for fault protection [10] and physical layer monitoring), service signals (e.g., for indicating slot reservation for synchronous data transfer) and, as studied in this paper, a bit/slot synchronization signal.

Work partially funded by Ministero dell'Istruzione, dell'Università e della Ricerca (MIUR), Italy, under PRIN project *WONDER* and by European Union under FP6 Network of Excellence *e-Photon/ONe*.

This full text paper was peer reviewed at the direction of IEEE Communications Society subject matter experts for publication in the IEEE ICC 2006 proceedings.

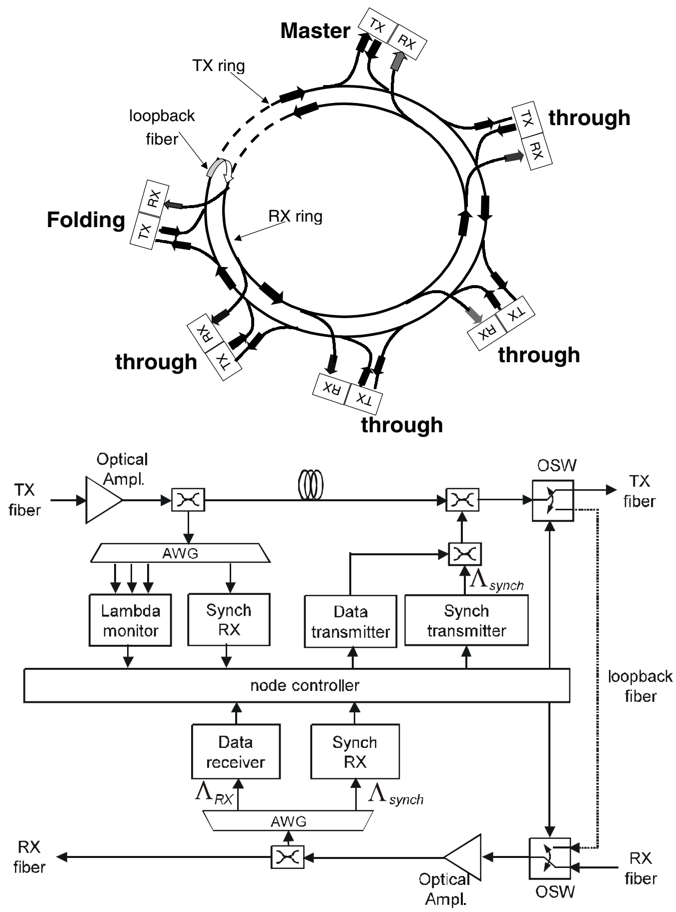

Fig. 1: WONDER network and node architecture.

Due to space limitation, only the main features of the network and node architecture can be outlined here. Fur further detail, on network design and experimental activity, the interested reader is referred to the cited papers [7][9][10].

As far as network synchronization is concerned, the most straightforward approach consists in distributing a timing signal on the dedicated wavelength. In this case, the first node of the folded bus (master node) transmits a periodic synchronization signal (e.g., pulses) on the control wavelength of the TX fiber, while every other node receives this signal on the RX fiber. Moreover, each node has a "Λ-monitor" capability on the TX fiber, which allows the node to sense the presence/absence of data signals (formatted as data packets) on each wavelength at every time slot.

The slot synchronization aim is enabling the transmitting nodes to insert packets ideally at the center of (empty) time slots. Misalignment on slot boundaries may ultimately lead to packet transmission on the border between adjacent time slots, thus leading to packet collisions and finally to data loss.

III. Network Model and Assumptions

The network model is characterized by the following parameters.

- N: number of network nodes, numbered as $j = 1, 2, \ldots, N$.
- W: number of data wavelengths used to transmit packet. Since $N = W$ is assumed (i.e., every node uses a unique optical channel to receive data), then node j receives packets only on the wavelength Λ_j.
- T_S: (ideal) time-slot interval (in our simulations, we have set $T_S = 1$ µs).
- T_P: packet transmission time ($T_P = 0.9$ µs) (considered constant in each node and in each time slot, independently from node clock error).
- L: fiber length between adjacent nodes.
- l: delay fiber length used in every node.
- F: length of the folding fiber used in the last node of the network to link transmission fiber and reception fiber.
- Wavelength spacing: $\Delta\lambda = 0.8$ nm. Chromatic dispersion coefficient: 16 ps/km·nm (12.8 ps/km).
- $t_{k,j}$: instant in which node j receives the signal indicating the beginning of k-th time slot.
- $TE_{k,j}$: random time error (TE) of time slot synchronization signal [11]; this value represents the time difference between the ideal reference (pulses received deterministically every µs) and the real reference for node j at slot k.

Each node stores packets received from clients in a logical queue. The client packet arrival process is modeled as a Poisson process: interarrival times at node i are exponentially distributed with average rate λ_i packets/slot. Client packets are addressed to other nodes uniformly, with average transmission rate $R_{i,j}$ from node i to node j [packets/slot]:

$$R_{i,j} = \lambda_i \cdot \frac{1}{N-1} \quad , \quad R_{i,i} = 0 \qquad (1).$$

Distributing time slot synchronization to network nodes, as most accurately as possible, is a key objective. Every node is expected to know exactly the beginning of each time slot on both TX and RX fibers. This information is not essential on RX: in fact, nodes are capable of receiving packets with their burst mode packet receiver and this operation is possible without knowing that in the next slot a packet will arrive.

On the TX fiber, at the beginning of each time slot, nodes perform the following operations:

- sampling the data channels (with the Λ-monitor function) in order to determine the idle or busy condition of each wavelength for the transmission in that time slot;
- transmission of a packet on one of the available wavelengths; the MAC is based on a proper queuing strategy.

The packet transmission time has been chosen $T_P = 0.9 \cdot T_S$. Thus, a guard time $T_G = 0.1 \cdot T_S$ is left to compensate limited time errors and chromatic dispersion.

Allowing a guard time does affect Λ-monitor operation. In fact, sampling the data channel too soon (just after the slot start) yields high probability that, due to time error and chromatic dispersion, the optical power on one or more wavelengths is not detected. This can lead to detect erroneously one or more wavelengths as idle, in spite of them being actually busy, thus causing a collision when these wavelengths are used by the node for packet transmission.

In order to avoid these collisions, every node has to sample data channels with a certain delay (Channel Probing Delay, D_p) after the beginning of the time slot. If every node samples data channels at the middle point of the time slot, i.e.

$D_p = 0.5$ µs (assumption made in all our study), the probability of avoiding detection errors due to time error and chromatic dispersion is minimized. However, this yields an additive delay of half time slot and also the presence of a longer fiber delay line in each station (used also to take into account the unavoidable electronic processing time of MAC operations).

In the next sections, two different time slot synchronization techniques for the WONDER ring are described. In the former, a slot synchronization signal is transmitted by the master station on a dedicated control wavelength. In the latter, slave nodes achieve slot synchronization aligning on data packets received from the master. For both of them, performance has been evaluated by simulation and advantages and drawbacks are outlined.

IV. Synchronization Signal Transmitted on Dedicated Control Wavelength

In this case, $W+1$ wavelengths are used: $W = N$ data channels and one additional dedicated channel to carry the synchronization signal. In this scenario, the first node on the transmission fiber is the master node: it transmits a timing signal that propagates along the fiber indicating to all other stations the start of time slots. Every slave node needs to receive this slot synchronization signal: thus, the generic node j has a receiver not only for wavelength Λ_j (on RX fiber) but also for control wavelength Λ_C (on TX fiber).

Ideally, the signal transmitted from the master on Λ_C is a series of pulses spaced 1 µs, which is detected without timing error by every station: no collisions happen. In a real scenario, several impairments can take place: the master station clock is subject to phase and frequency deviations [11], the generic slave node probes the received signal and begins packet transmission a bit sooner or a bit later than expected, the processing time required by MAC operations is different from that added by the fiber delay line. These effects contribute to make network nodes affected by time error and to make packet collisions more frequent due to time-slot misalignment.

Also chromatic dispersion plays an important role in slot synchronization, as it causes packets transmitted on different wavelengths to propagate at different speeds. For this reason, packets transmitted on different wavelengths arrive to destination shifted from ideal time alignment. In order to reduce the negative effect of chromatic dispersion, it has been chosen to have the control wavelength (which is supposed with propagation speed $v = 2\cdot10^{-8}$ m/s) as the "central wavelength" between data channels.

Given the parameters defined previously, we can express the slot synchronization time $t_{k,j}$ at node j for slot k as

$$t_{k,j} = kT_S + (j-1)\cdot\frac{(L+l)}{v} + TE_{k,j} \quad (2).$$

The term $(j-1)(L+1)/v$ is the propagation delay. $TE_{k,j}$ is the random time error that, combined with chromatic dispersion, could cause packet collision. In all our simulations, the effect of chromatic dispersion has been taken into account, although not explicitly indicated in this and following formulas.

In our model, $TE_{k,1}$ is the random time error series of the first clock in the chain, i.e. the master node. As far as the other nodes ($j>1$, slave nodes) are concerned, we considered two possibilities: a simple model, in which each slave node simply detects pulses on the control wavelength and is affected by random trigger error, and a Phase-Locked Loop (PLL) model, in which slave clocks behave as a PLL that tracks the timing signal transmitted by the master.

In the simple model:

- in a given time slot k, the values $TE_{k,j}$ are independent (i.e., TE samples in the same time slot at different nodes are uncorrelated);
- in a given node j, the values $TE_{k,j}$ are independent (i.e., no time correlation is assumed in TE sequences at every node);
- the random variables $TE_{k,j}$ have uniform probability distribution in interval $(-\sqrt{3}\sigma, +\sqrt{3}\sigma)$, where σ is the distribution standard deviation.

In the PLL model, the PLL low-pass filters phase fluctuations of the synchronization signal on the control wavelength [11]. PLL internal noise comes mainly by two sources: one by the Voltage-Controlled Oscillator (VCO) and another by the phase detector and the loop filter [11][12]. The former noise is high-pass filtered to the output signal, whereas the latter is low-pass filtered**.** We neglected the VCO noise, because quartz oscillators are very stable in the short term. On the other hand, we modeled the phase detector and loop filter noise with the random time error series $TE_{k,j}^{\mathrm{DF}}$, where:

- in a given time slot k, the values $TE_{k,j}^{\mathrm{DF}}$ are independent;
- in a given node j, the values $TE_{k,j}^{\mathrm{DF}}$ are independent;
- the random variables $TE_{k,1}$ have uniform probability distribution in $(-\sqrt{3}\sigma_{\mathrm{M}}, +\sqrt{3}\sigma_{\mathrm{M}})$, where σ_{M} is the standard deviation of the random time error on the master clock;
- the random variables $TE_{k,j}^{\mathrm{DF}}$ have uniform probability distribution in $(-\sqrt{3}\sigma_{\mathrm{DF}}, +\sqrt{3}\sigma_{\mathrm{DF}})$, where σ_{DF} is the standard deviation of the random time error generated at the PLL phase detector and loop filter.

The 2$^{\text{nd}}$ and 4$^{\text{th}}$ assumptions reflect what may be expected from a digital PLL with quantizer-like phase detector.

We assumed the classic linear baseband model of 2$^{\text{nd}}$-order PLL with active loop filter (perfect integrator) [11], having input-output phase transfer function

$$H(s) = \frac{\phi_{\mathrm{OUT}}(s)}{\phi_{\mathrm{IN}}(s)} = \frac{2\zeta\omega_{\mathrm{N}}s + \omega_{\mathrm{N}}^2}{s^2 + 2\zeta\omega_{\mathrm{N}}s + \omega_{\mathrm{N}}^2} \quad (3)$$

where ζ is the damping ratio (we assumed $\zeta = 1$) and ω_{N} is the natural angular frequency. Therefore, the time error series at each node j are given by

$$TE_{k,j} = \begin{cases} TE_{k,1} & j = 1 \\ TE_{k,1} * h(k) + TE_{k,j}^{\mathrm{DF}} * h(k) & j = 2, 3, ..., N \end{cases} \quad (4)$$

where $h(k)$ is the impulse response corresponding to $H(s)$.

We have evaluated the network performance for different values of the natural frequency $f_{\mathrm{N}} = \omega_{\mathrm{N}}/2\pi$, for both the simple and PLL models. We remark that, in the PLL linear baseband model (3), the cut-off (-3 dB point) frequency B is proportional to its natural frequency, as

$$B = \frac{\omega_N}{2\pi}\sqrt{2\zeta^2 + 1 + \sqrt{(2\zeta^2+1)^2+1}} \qquad (5).$$

With $\zeta = 1$, we have $B \cong 2.48 \cdot f_N$.

All simulations have been run repeatedly, independently, until 95%-confidence intervals less than 5% of the collision probability estimate were attained. The discrete-event simulator was realized in OMNeT++ [13].

Fig. 2 compares the packet collision probability (average on all nodes) with timing signal on dedicated control wavelength, with and without a PLL in each node, with uniform packet arrival rate λ_i = 0.9 packets/slots.

Generally, using PLLs improves the network performance, especially when B is sufficiently low. Nevertheless, we observe that the simple model may achieve better performance in few cases, i.e. when B is high and the TE standard deviation σ_M of the master node is low. Moreover, while the collision probability decreases with B for small σ_M, the opposite behavior is observed for high values of σ_M. This is caused by the velocity at which PLLs follow input phase fluctuations: if B is high, this velocity is high, although internal noise in not filtered out much. For high input noise, this last phenomenon prevails and yields lower collision probability.

The design of a network with a PLL in each slave node would require knowing the maximum standard deviation of the master time error (σ_M) and of the internal time error (σ_{DF}) that could be tolerated, in order to have collision probability lower than a given limit. Figs. 3 and 4 provide such information for a given collision probability ($P_C = 10^{-6}$) and PLL natural frequency (f_N = 12.5 kHz, $B \cong$ 31 kHz).

Fig. 3 shows that TE requirements are more severe with higher PLL cut-off frequency B. The lower is B, the more the noise power is filtered out and thus the working area in the graph (below the curve) becomes bigger.

Moreover, Figs. 3 and 4 show the asymmetry of the curves. The master random time error adversely affects the collision probability more than the random time error in the PLL phase detector and loop filter. This asymmetry vanishes if f_N is high (e.g., 50 kHz). From Fig. 4, we note also that the asymmetry of the curves is larger for higher collision probability.

V. Synchronization on Data Packets from The Master

Slot synchronization based on transmitting a timing signal on a dedicated control wavelength, although granting good performance, has two important drawbacks:

- need of one additional wavelength;
- need of one additional receiver on TX fiber in every node (except the master).

Thus, in order to reduce the network cost, we envisaged an alternative slot synchronization technique, based on aligning on arrival times of data packets transmitted by the master. In this method, it is assumed to know, in each node, the fixed delay from the slot on TX and the slot on RX.

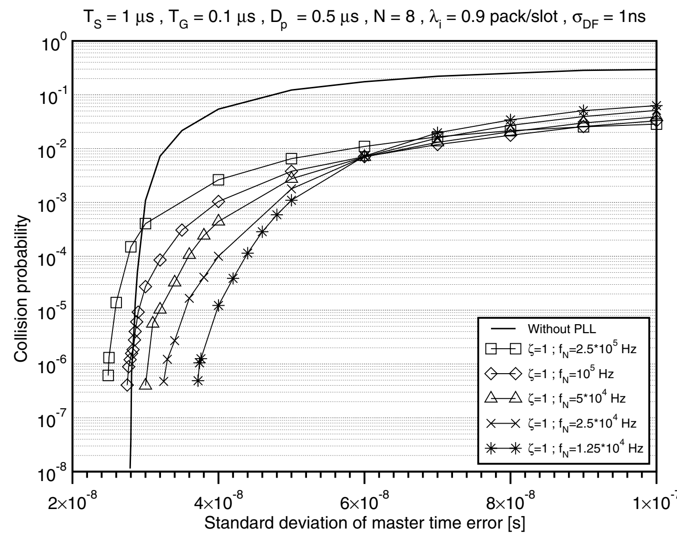

Fig. 2: Collision probability with timing signal on dedicated control wavelength (simple model vs. PLL model).

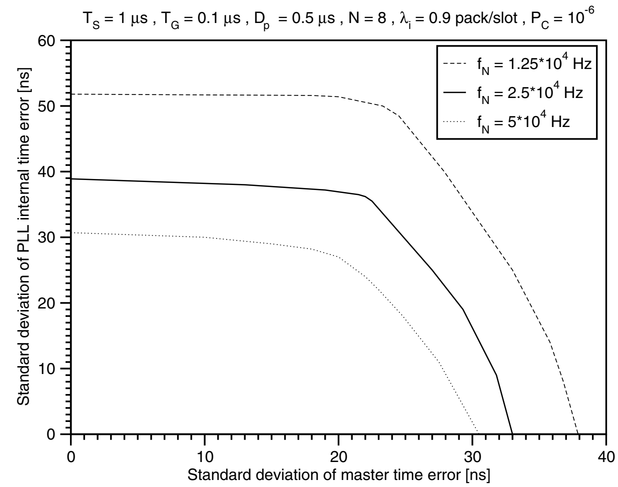

Fig. 3: Standard deviations σ_M (noise from master clock) and σ_{DF} (noise from PLL phase detector and loop filter) for fixed collision probability $P_C = 10^{-6}$ and PLL natural frequency f_N.

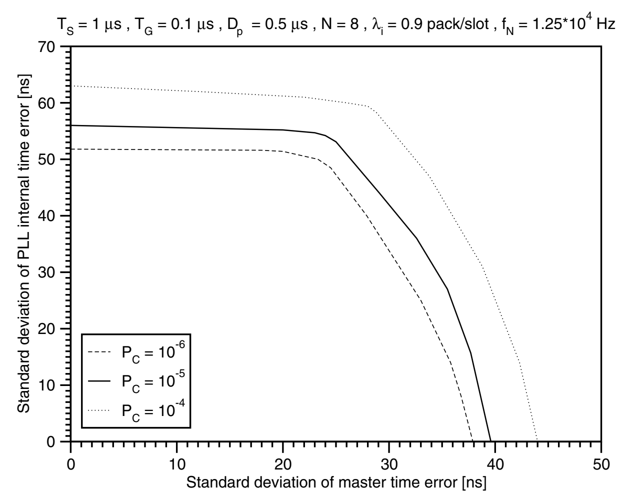

Fig. 4: Standard deviations σ_M (noise from master clock) and σ_{DF} (noise from PLL phase detector and loop filter) for fixed collision probability P_C and PLL natural frequency f_N=12.5 kHz.

This full text paper was peer reviewed at the direction of IEEE Communications Society subject matter experts for publication in the IEEE ICC 2006 proceedings.

In this scenario, the master node is not necessarily the first node on the TX fiber. The master is assumed to have an ideal clock, which every microsecond chimes time slots and triggers the transmission of data packets. When a node receives a packet from the master (the packet header includes sender information), it determines (with error because based on a non-ideal clock) the beginning of the successive slot on the TX fiber adding the fixed delay. However, let us to point out that slave nodes do not receive a packet from the master every slot: when they do not, they evaluate the next slot start time on TX based on their inaccurate clock. Now, we remark that:

- slave nodes get synchronized by the arrival of data packets from the master; on packet arrival, they align their clock current phase to the master clock, not necessarily in the next slot but possibly in one of the following slots, if delay from reception to transmission is too short;
- the contribution of chromatic dispersion can be estimated in advance and used to correct clock realignment after reception of data packets.

To model slot synchronization on data packets from the master, two vectors have been defined:

- $\mathbf{r}_j^{\mathrm{M}} = \{ r_{i,j}^{\mathrm{M}} \}$: time instants in which node j receives packet i from the master ($j = 1, 2, \ldots, N$; $i = 1, 2, \ldots$);
- $\mathbf{t}_j^{\mathrm{M}} = \{ t_{i,j}^{\mathrm{M}} \}$: time instants in which node j schedules the beginning of time slot i on TX, based on timing of data packets received from the master ($j = 1, 2, \ldots, N$; $i = 1, 2, \ldots$).

The start instant of time slots is computed by the generic slave node j (node 1 identifies the master) as:

$$t_{k,1} = kT_{\mathrm{S}} \tag{6}$$

$$t_{0,j} = t_{1,j}^{\mathrm{M}} + TE_{0,j} \tag{7}$$

$$t_{k,j} = t_{i,j}^{\mathrm{M}} + TE_{k,j} \qquad \text{if } \exists i \,\middle|\, t_{k\text{-}1,j} \le r_{i,j}^{\mathrm{M}} < t_{k-1,j} + T_{\mathrm{S}} + TE_{k,j} \tag{8}$$

$$t_{k,j} = t_{k-1,j} + T_{\mathrm{S}} + TE_{k,j}$$
$$\text{if } \nexists \mathrm{i} \,\middle|\, t_{k\text{-}1,j} \le r_{i,j}^{\mathrm{M}} < t_{k-1,j} + T_{\mathrm{S}} + TE_{k,j} \tag{9}$$

We point out that here slot numbering is not global, like in eq. (2), because for each node the first slot begins after reception of the first packet from the master. The formulas above mean that (the fixed delay has not been indicated explicitly):

- the master has ideal clock (6);
- each node waits for the first packet from the master to begin transmission (7);
- when a node receives a packet from the master, it determines the next transmission instant adding the fixed delay between slots on TX and RX fibers (8);
- when a node does not receive it, it determines the beginning of the next time slot on TX fiber using its (inaccurate) internal clock (9).

It is evident that network synchronization performance depends strongly on the average rate λ_{M}, with which packets are received from the master. To verify it, this synchronization method has been simulated over 20000 time slots, according to relationships (6)—(9). For the sake of simplicity, $TE_{k,j}$ samples have been assumed uncorrelated and distributed uniformly in interval $(-\sqrt{3}\sigma, +\sqrt{3}\sigma)$, with standard deviation $\sigma = 10$ ns.

Under this simple assumption, if the slave node can never align on data packets received from the master (i.e., $\lambda_{\mathrm{M}} = 0$), its cumulative time error wanders unlimited. Actually, this result is what, in random process theory, is called *random walk* (i.e., integral of white noise): continuous summation of independent increments (random time error samples).

Fig. 5 shows the cumulative time error sequence obtained by simulation for $\lambda_{\mathrm{M}} = 0$. The standard deviation of this sequence results $\sigma_{\mathrm{CUM}} = 240$ ns. Note that the variance of a random walk, defined by infinite-time averaging, is infinite. Thus, the value σ_{CUM} actually depends on the sequence length.

The more often a node can align its time scale on the arrival times of data packets from the master, the lower will be the standard deviation of its cumulative time error. For example, Figs. 6 and 7 show the time error cumulated by a slave node when $\lambda_{\mathrm{M}} = 0.1$ ($\sigma_{\mathrm{CUM}} = 84$ ns) and $\lambda_{\mathrm{M}} = 0.9$ ($\sigma_{\mathrm{CUM}} = 29$ ns).

Finally, simulation results shown in Fig. 8 show how collision probability (average on all nodes) decreases by increasing λ_{M}, with same parameter setting as before. We note that the synchronization technique based on dedicated control wavelength performs better than the method of synchronizing on data packets from the master, for all λ_{M} values considered.

VI. Conclusions

In this paper, we studied two different strategies of slot synchronization in WDM packet-switched slotted rings networks: in the former, a slot synchronization signal is transmitted by the master station on a dedicated control wavelength; in the latter, slave nodes achieve slot synchronization aligning on data packets received from the master. Emphasis has been given to the architecture of the WONDER network, currently under experimental development. The performance of the two synchronization strategies has been evaluated by simulation.

We found that the technique based on transmitting a timing signal on a dedicated control wavelength achieves good performance in terms of packet collision probability, especially if every node tracks the timing reference by means of a PLL, which low-pass filters the phase fluctuations on the timing signal transmitted by the master node.

In the WONDER project, it has been chosen to dedicate a wavelength channel to synchronization distribution. As mentioned in Sec. II, dedicating a wavelength to service purposes allows a variety of additional functions, such as support of fault protection, indicating slot allocation for synchronous data transfer, detection of faults. Moreover, on the control channel a more complex synchronization signal may be transmitted, distributing not only slot timing but also bit frequency, to aid burst-mode receivers in bit timing acquisition.

Alternatively, aligning on data packets from the master allows saving the cost of the additional control wavelength and associated receivers. Nevertheless, this technique attains worse slot synchronization performance. Actually, each node is timed by the internal inaccurate clock between master packet arrivals. Moreover, the synchronization performance is strongly dependent on the master packet transmission rate.

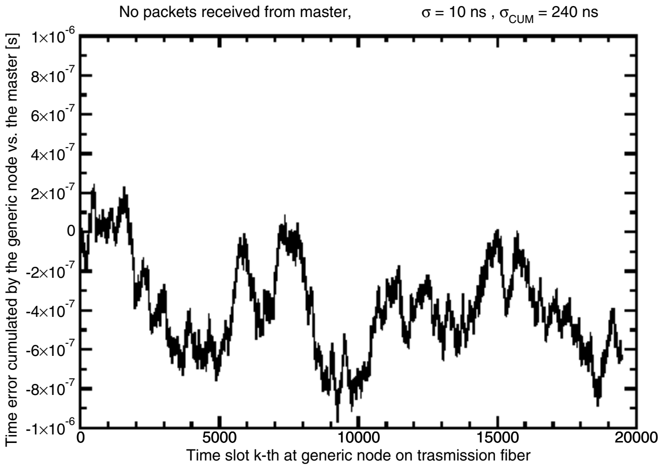

Fig. 5: Cumulative time error in a slave node with no data packets from the master (λ_M=0 packets/slot).

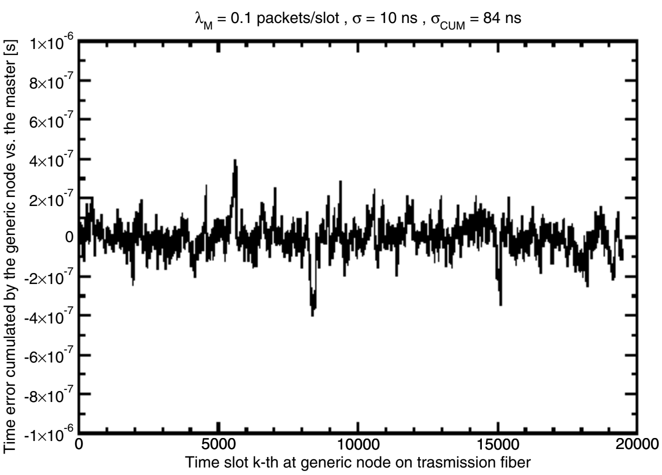

Fig. 6: Cumulative time error in a slave node aligning on data packets from the master (λ_M=0.1 packets/slot).

However, this technique, yet attaining lower timing stability, still deserves further study, especially if limiting the number of wavelengths and of receivers is a strong requirement.

The results obtained in this work have been useful in the design of the WONDER network. However, they have also general interest, since similar architectures of optical packet-switched slotted ring networks gather significant attention in optical networking research.

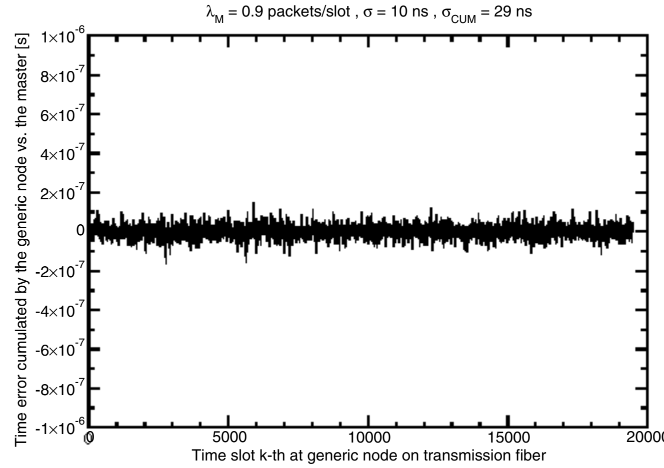

Fig. 7: Cumulative time error in a slave node aligning on data packets from the master (λ_M=0.9 packets/slot).

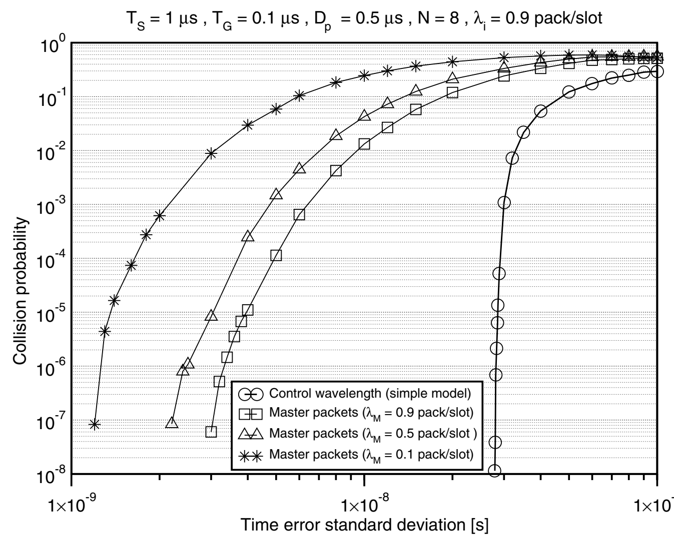

Fig. 8: Collision probability with synchronization on data packets from the master, compared to synchronization on dedicated control wavelength.

REFERENCES

[1] B. Mukherjee, *"Optical Communication Networks"*. New York, USA: McGraw-Hill, 1997.

[2] C. S. Jelger, J. M. H. Elmirghani, "Photonic Packet WDM Ring Networks Architecture and Performance", *IEEE Communications Magazine*, 40(11):110-115, Nov. 2002.

[3] M. Herzog, M. Maier, and M. Reisslein, "Metropolitan Area Packet-Switched WDM Networks: A survey on Ring Systems," *IEEE Commun. Surv.*, vol. 6, no. 2, pp. 2–20, 2nd Quarter 2004.

[4] M. Ajmone Marsan, A. Bianco, E. Leonardi, M. Meo and F. Neri, ``MAC Protocols and Fairness Control in WDM Multi-Rings with Tunable Transmitters and Fixed Receivers", IEEE/OSA Journal on Lightwave Technology, Vol. 14, No. 6, pp. 1230-1244, Jun.1996.

[5] H.-S. Yang, M. Herzog, M. Maier, M. Reisslein, "Metro WDM Networks: Performance Comparison of Slotted Rings and AWG Star Networks", *IEEE J. Select. Areas Commun.*, 22(8): 1460-1473, Oct. 2004.

[6] K. V. Shrikhande, I. M. White, D. Wonglumsom, S. M. Gemelos, M. S. Rogge, Y. Fukashiro, M. Avenarius, and L. G. Kazovsky, ``HORNET: a packet-over-WDM multiple access metropolitan area ring network", IEEE Journal on Selected Areas in Communications, Vol. 18, No. 10, pp. 2004-2016, Oct. 2000.

[7] A. Carena, V. De Feo, J. Finochietto, R. Gaudino, F. Neri, C. Piglione, P. Poggiolini, "RingO: An Experimental WDM Optical Packet Network for Metro Applications", IEEE Journal on Selected Areas in Communications, Vol. 22, Issue 8, pp. 1561-1571, Oct. 2004.

[8] Ministero dell'Istruzione, dell'Università e della Ricerca della Repubblica Italiana, PRIN Programme 2003, Project WONDER (WDM Optical Network DEmonstrator over Rings). Partners: Politecnico di Torino, Politecnico di Milano, Università di Parma.

[9] A. Bianciotto and R. Gaudino, ``WONDER: overview of a packet-switched MAN architecture", OpNeTec 2004, Pisa, Italy, Oct. 2004.

[10] A. Bianciotto, J. Finochietto, R. Gaudino, F. Neri, C. Piglione, A. Samperi, "Fast and efficient fault-recovery strategies in the WONDER metro architecture", NOC 2005, London, UK, July 2005.

[11] S. Bregni, "Chapter 5 - Characterization and Modelling of Clocks", in *Synchronization of Digital Telecommunications Networks*. Chichester, UK: John Wiley & Sons, 2002, pp. 203-281.

[12] V. F. Kroupa, "Noise Properties of PLL Systems", *IEEE Trans. Commun.*, 30(10): 2244-2252, Oct. 1982.

[13] OMNeT++ Discrete Event Simulation System. Available: http://www.omnetpp.org.